Optical Engineering

OpticalEngineering.SPIEDigitalLibrary.org

Stress measurement of thin film on flexible substrate by using projection moiré method and heterodyne interferometry

Kun-Huang Chen
Jing-Heng Chen
Hua-Ken Tseng
Wei-Yao Chang

SPIE.

Kun-Huang Chen, Jing-Heng Chen, Hua-Ken Tseng, Wei-Yao Chang, "Stress measurement of thin film on flexible substrate by using projection moiré method and heterodyne interferometry," *Opt. Eng.* **55**(6), 064102 (2016), doi: 10.1117/1.OE.55.6.064102.

Optical Engineering 55(6), 064102 (June 2016)

Stress measurement of thin film on flexible substrate by using projection moiré method and heterodyne interferometry

Kun-Huang Chen,[a,*] Jing-Heng Chen,[b] Hua-Ken Tseng,[a] and Wei-Yao Chang[c]
[a]Feng Chia University, Department of Electrical Engineering, 100 Wenhwa Road, Seatwen, Taichung 40724, Taiwan
[b]Feng Chia University, Department of Photonics, 100 Wenhwa Road, Seatwen, Taichung 40724, Taiwan
[c]National Chiao-Tung University, Department of Photonics and Institute of Electro-Optical Engineering, 1001 Ta-Hsueh Road, Hsinchu County 30050, Taiwan

Abstract. We propose a stress measurement system based on a projection moiré method and heterodyne interferometry for thin films on a flexible substrate. In the measurement setup, a CMOS camera in which every pixel can receive a series of heterodyne moiré signals by using a continuously relative displacement with a constant velocity is used. Furthermore, the phase of the optimized sinusoidal curve and the surface profile of the flexible substrate are determined using a least-squares sine fitting algorithm. The thin-film stress is obtained by representing the cross-sectional curve of the surface profile by using a polynomial fitting method, estimating the resultant curvature radii of the uncoated and coated substrates, and using these two radii in the corrected Stoney formula. The proposed measurement system has the advantages of high accuracy, high resolution, and high capacity for substrates with high flexibility and a large measurement depth. [DOI: 10.1117/1.OE.55.6.064102]

Keywords: flexible substrate; thin-film stress measurement; projection moiré; Talbot effect; heterodyne interferometry.

Paper 160224P received Feb. 22, 2016; accepted for publication May 5, 2016; published online Jun. 1, 2016.

1 Introduction

The increased demand for light, thin, and flexible electronic devices has caused the flexible electronics industry to grow; examples of such devices are flexible displays,[1,2] electronic skin,[3] flexible luminance,[4,5] flexible solar cell,[6,7] and biologic sensor.[8,9] Because flexible substrates on which thin films are fabricated are affected by the stress associated with the fabrication process, the measurement and analysis of thin-film stress are crucial for fabricating and developing flexible electronic devices. Furthermore, in flexible substrates coated with a noncrystalline thin film, the thin-film stress can cause large deformations, and, therefore, conventional testing techniques, such as optical interferometry[10–13] and x-ray diffraction method,[14,15] cannot be used. The moiré method involves a large measurement depth, high stability, and a simple and economical optical configuration, and, therefore, it is considered appropriate for the stress measurement of thin films on flexible substrates. Lee et al.[16] and Huang and Lo[17] proposed the methods for measuring the stress in thin films on flexible substrates; the methods involve using the shadow moiré method and analyzing the interval between the moiré fringes. The resolution and accuracy of these methods are not high because only the maximum and minimum of the moiré fringes are measured for determining the fringe contours, and, therefore, the resolution and accuracy can be strongly affected by the uneven spatial distribution of the light intensity. Accordingly, we propose a stress measurement system for thin films on flexible substrates. An expanded and collimated laser light is passed through a linear projection grating to form a self-image of the grating on a flexible test substrate, and the resultant deformed fringes are obtained on a reference grating to generate moiré fringes that are recorded by a CMOS camera. When the projection grating is moved with a constant velocity in the grating plane, every pixel of the CMOS camera records a series of signals that mimic a heterodyne interferometric signal. Therefore, the phase of the signals can be extracted in a manner identical to that of obtaining the phase of heterodyne interferometric signals. The phases of the optimized sinusoidal curves can be calculated using a least-squares sine fitting algorithm. The phase distribution and resultant surface profile of the uncoated and coated flexible substrates can be reconstructed by employing phase unwrapping and a derived equation. Subsequently, polynomial curve fitting is used to determine the curvature radii of the uncoated and coated flexible substrates, and these radii are used in the corrected Stoney formula for obtaining the thin-film stress. This method has the advantages of high stability and high resolution because of the use of the projection moiré method and heterodyne interferometry.

2 Principle

Figure 1 shows the optical configuration in the proposed method. For convenience, the observation axis of the CMOS camera is considered to be the z-axis, and the y-axis is directed perpendicular to the plane of the paper. A laser beam of wavelength λ is passed through a beam expander (BE) for expanding and collimating the beam, and then it impinges on a projection grating G_1 at an angle θ to form a self-image of G_1 on the flexible test substrate. The self-image distance Z_1 can be expressed as[18]

*Address all correspondence to: Kun-Huang Chen, E-mail: chenkh@fcu.edu.tw

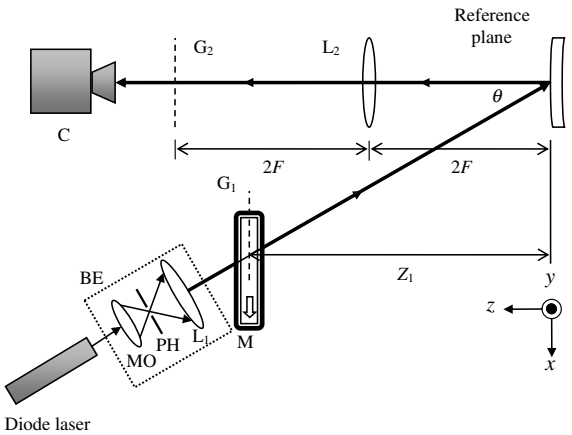

Fig. 1 Optical configuration in the proposed method. BE: beam expander; MO: objective; PH: pinhole; L_1: collimating lens; L_2: imaging lens; L_3: camera lens; G_1 and G_2: linear gratings; M: motorized translation stage; C: CMOS camera; Z_1: first self-image; and F: focal length of the imaging lens.

$$Z_1 = \frac{p^2}{\lambda}\cos^3\theta, \tag{1}$$

where p denotes the pitch of G_1. The projected fringes of the self-image can be distorted because of the flexibility of the substrate. These distorted fringes are imaged on the reference grating G_2 of the same pitch with G_1 via a camera lens to form the moiré fringes and captured by the CMOS camera C. The recorded fringe image can be expressed as[19]

$$I(x,y) = \frac{1}{4}\left\{1 + \cos\left[\frac{2\pi}{p}x + \Psi(x) + \varphi_1\right] + \cos\left(\frac{2\pi}{p}x + \varphi_2\right) + \frac{1}{2}\cos\left[\frac{4\pi}{p}x + \Psi(x) + \varphi_1 + \varphi_2\right] + \frac{1}{2}\cos[\Psi(x,y) + \varphi_1 - \varphi_2]\right\}, \tag{2}$$

where ϕ_1 and ϕ_2 denote the initial phase of G_1 and G_2. Furthermore, $\Psi(x)$ is the phase of the height distribution $S(x)$ on the substrate and can be written as

$$\Psi(x) = \frac{2\pi}{p}S(x)\tan\theta. \tag{3}$$

In Eq. (2), the second, third, and fourth terms represent the harmonic noise, and the final term describes the desired moiré fringes formed on the surface of the flexible substrate. Hence, the moiré fringes can be obtained by filtering the harmonic noise, and the intensity of the moiré fringe image can be written as

$$I'(x,y) = I_0(x,y) + \gamma(x,y)\cos[\Psi(x) + \phi_1 - \phi_2], \tag{4}$$

where I_0 denotes the average light intensity, $\gamma(x,y)$ denotes the visibility, and $\phi_1 - \phi_2$ is the initial phase difference. When the motorized translation stage M, on which G_1 is mounted, is moved along the x-axis at constant velocity v for time t, every pixel of the CMOS camera can receive a continuous sinusoidal signal, whose intensity can be expressed as

$$I'(x,y) = I_0(x,y) + \gamma(x,y)\cos[2\pi f t + \Psi(x)], \tag{5}$$

where $f(=v/p)$ denotes the heterodyne moiré frequency associated with the time-varying phase. According to Eq. (3), $S(x)$ can be expressed as

$$S(x) = \frac{p}{2\pi\tan\theta}\Psi(x). \tag{6}$$

According to this equation, the surface profile corresponding to $S(x)$ can be reconstructed by measuring the phase $\Psi(x)$.

To determine $\Psi(x)$, Eq. (5) can be rewritten as

$$I'(x,y) = A\cos(2\pi f t) + B\sin(2\pi f t) + C, \tag{7}$$

where A, B, and C are the real numbers. Moreover,

$$\Psi(x,y) = \tan^{-1}\left(\frac{-B}{A}\right). \tag{8}$$

Accordingly, the phase of the moiré fringes on a single pixel can be calculated using a least-squares sine fitting algorithm to obtain A and B. The parameter $\Psi(x)$ can be obtained by following the aforementioned procedures for the other pixels and unwrapping the obtained phases, and the surface profile can subsequently be reconstructed using Eq. (6).

To obtain the curvature radius of the substrate, the cross-sectional curve (Fig. 2) of the reconstructed surface profile in the x-direction and passing through the image center was obtained by using a polynomial fitting method. Let the center of the curve be set as (x_0, h_0), and let (x_1, h_1), (x_2, h_2), and (x_3, h_3) be three points on the curve. The three circular equations can then be expressed as

$$(x_1 - x_0)^2 + (h_1 - h_0)^2 = R^2, \tag{9}$$

$$(x_2 - x_0)^2 + (h_2 - h_0)^2 = R^2, \tag{10}$$

$$(x_3 - x_0)^2 + (h_3 - h_0)^2 = R^2, \tag{11}$$

where R is the curvature radius. Let $x_1 - x_2 = L$, $h_2 - h_1 = \delta_1$, $x_2 - x_3 = L$, and $h_3 - h_2 = \delta_2$, where L is an arbitrary value. The curvature radius can then be derived as

$$R = \sqrt{\left[\frac{(\delta_1+\delta_2)(\delta_1\delta_2 + L^2)}{2L(\delta_1 - \delta_2)}\right]^2 + \left[\frac{(2L^2 + \delta_1^2 + \delta_2^2)}{2(\delta_1 - \delta_2)}\right]^2}. \tag{12}$$

When L, δ_1, and δ_2 are known, R can be obtained from Eq. (12). Furthermore, the corrected Stoney formula for obtaining the stress in thin films on flexible substrates can be expressed as[16]

$$\sigma_f = \frac{(Y_s t_s^2 - Y_f t_f^2)^2 + 4Y_s Y_f t_s t_f (t_s + t_f)^2}{6(1+\nu)Y_s Y_f t_s t_f (t_s + t_f)} \frac{Y_f^*}{\left(1 + \frac{Y_f^* t_f}{Y_s^* t_s}\right)}\left(\frac{1}{R} - \frac{1}{R_0}\right), \tag{13}$$

where σ_f denotes the thin-film stress, t_s and t_f denote the thickness of substrate and thin film, respectively, $\nu = [(\nu_s + \nu_f)/2]$ denotes the average of the Poisson ratios of the

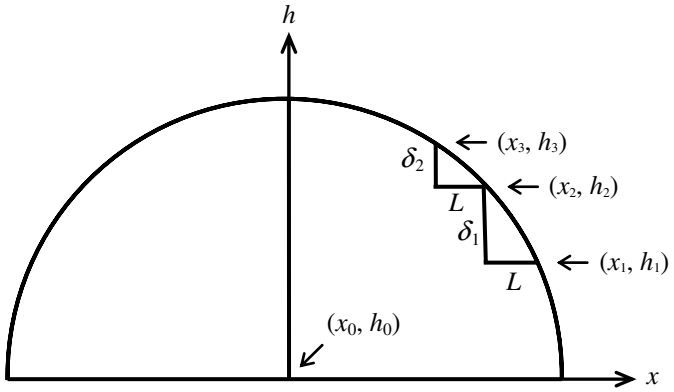

Fig. 2 Cross-sectional curve of the reconstructed surface profile in the x-direction and passing through the image center; (x_0, h_0) is the center of the curve, and (x_1, h_1), (x_2, h_2), and (x_3, h_3) are the three points on the curve.

substrate and thin film, Y_s and Y_f denote the elastic coefficients of the substrate and thin film, respectively, E_s and E_f denote the Young's moduli of the substrate and thin film, respectively, and R_0 denotes the curvature radius of the uncoated substrate. When these parameters are known, the desired thin-film stress can be obtained by reconstructing the surface profile by using the heterodyne moiré method, calculating the curvature radii R_0 and R, and using these curvature radii in Eq. (13).

3 Experimental Results and Discussion

To determine the validity of the proposed method, it was applied to a polyimide (PI)-coated flexible substrate. The surface of the PI-coated substrate was coated with a 100-nm thick indium tin oxide (ITO) thin film. The relative parameters of the PI substrate and ITO thin film are shown in Table 1. The experimental setup included a 473-nm diode laser, two linear gratings with a pitch of 0.2822 mm, an imaging lens with a focal length of 200 mm, a motorized translation stage [Sigma Koki/SGSP(MS)26-100] with a resolution of 0.05 μm for generating heterodyne moiré signals with a frequency (f) of 1 Hz ($v = 0.2822$ mm/s), and a CMOS camera (Basler/A504k) with an 8-bit gray level and a resolution of 1280×1024. The frame rate of the CMOS camera (f_s) was 15 fps, the exposure time (a) was 66 ms, and the total time (T) taken to record heterodyne moiré signals at different time points was 1 s. Every recorded moiré image was filtered using a 3×1 window through two-dimensional median filtering for eliminating the harmonic noise in the moiré fringes.[20] Figures 3 and 4 show the experimental results. Figures 3(a) and 4(a) show the moiré patterns on the sample with the uncoated and coated PI substrates. Figures 3(b) and 4(b) show the reconstructed surface profile of the PI substrate before and after thin-film coating. The cross-sectional curve of the reconstructed surface profile in the x-direction and passing through the image center is shown. Moreover, the fitting curve of the depicted cross-sectional curve can be obtained through polynomial curve fitting, as shown in Figs. 3(c) and 4(c). The parameters R_0 and R of the uncoated and coated substrates can be calculated as 182.7 and 51.3 cm by using Eq. (12). By substituting these values and the parameters in Table 1 into Eq. (13), the stress in the thin film on the PI substrate can be calculated as 43.8 MPa.

Table 1 Parameters of the PI substrate and ITO thin film.[21,22]

	PI substrate	ITO thin film
Thickness, t	$t_s = 75$ μm	$t_f = 100$ nm
Elastic coefficient, E	$E_s = 2.5$ GPa	$E_f = 116$ GPa
Poisson ratio, ν	$\nu_s = 0.34$	$\nu_f = 0.35$

According to Eq. (12), the error in the curvature radius in the proposed method can be expressed as

$$\Delta R = \left|\frac{\partial R}{\partial \delta_1}\right| \Delta\delta_1 + \left|\frac{\partial R}{\partial \delta_2}\right| \Delta\delta_2, \tag{14}$$

where $\Delta\delta_1$ and $\Delta\delta_2$ are equal and denote the errors in the height. Therefore, Eq. (14) can be rewritten as

$$\Delta R = 2\left|\frac{\partial R}{\partial \delta_1}\right| \Delta\delta_1 = 2\left|\frac{1}{2R}\frac{\partial R^2}{\partial \delta_1}\right| \Delta\delta_1. \tag{15}$$

The error in the curvature radius can be calculated as follows by using Eq. (15):

$$\Delta R = \frac{1}{R}\left[\frac{A\delta_1}{C^2} - \frac{A^2}{C^3} + \frac{BD^2}{2\ L^2C^2} + \frac{B^2D}{2\ L^2C^2} - \frac{B^2D^2}{2\ L^2C^3}\right]\Delta\delta_1, \tag{16}$$

where

$$A = 2L^2 + \delta_1^2 + \delta_2^2, \tag{17}$$

$$B = \delta_1 + \delta_2, \tag{18}$$

$$C = \delta_1 - \delta_2, \tag{19}$$

$$D = L^2 + \delta_1\delta_2. \tag{20}$$

and

$$\Delta\delta_1 = \left|\frac{\partial \delta_1}{\partial p}\Delta p\right| + \left|\frac{\partial \delta_1}{\partial \beta}\Delta\beta\right| + \left|\frac{\partial \delta_1}{\partial \theta_1}\Delta\theta_1\right| + \left|\frac{\partial \delta_1}{\partial \theta_2}\Delta\theta_2\right|, \tag{21}$$

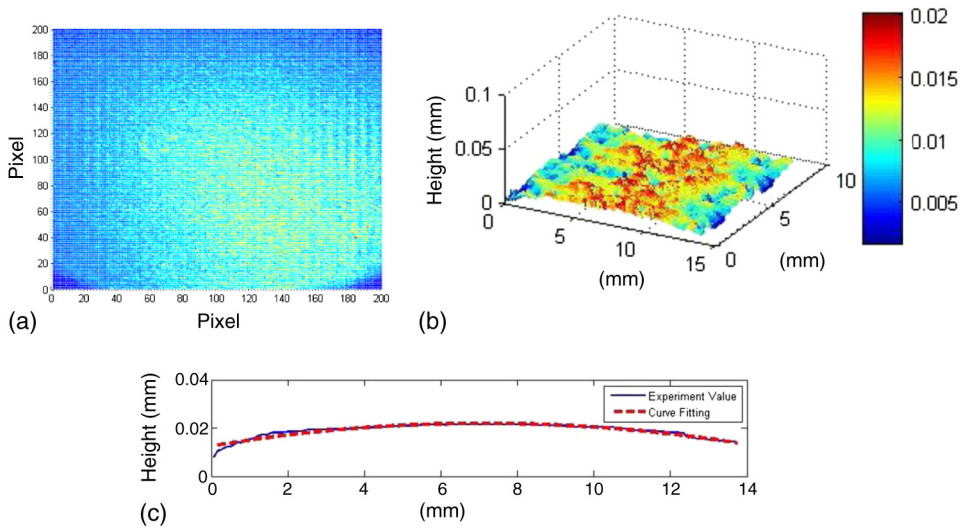

Fig. 3 Results for the uncoated PI substrate: (a) moiré pattern on the sample surface, (b) reconstructed surface profile, and (c) cross-sectional curve and fitting curve of the reconstructed surface profile.

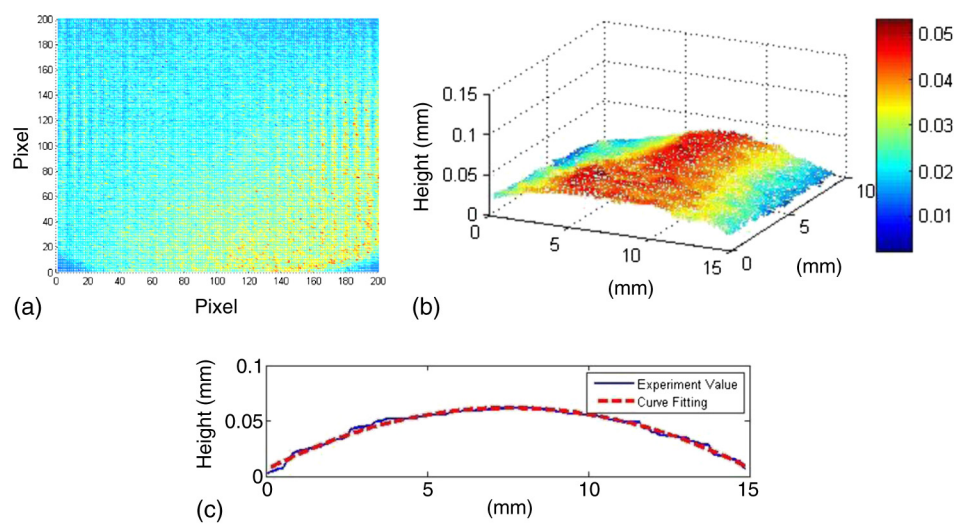

Fig. 4 Results for the coated PI substrate: (a) moiré pattern on the sample surface, (b) reconstructed surface profile, and (c) cross-sectional curve and fitting curve of the reconstructed surface profile.

where Δp, $\Delta\beta$, and $\Delta\theta$ denote the errors in the grating pitch, projection angle, and phase error, respectively. The error Δp originates from errors in the grating fabrication. The gratings were fabricated using a mask laser writer on a coated glass substrate, and Δp was estimated as 0.1 μm. The parameter $\Delta\beta$ originates from errors in the axis alignment. For a grating self-image of 110 mm and a projection angle of 30 deg in the experiment, $\Delta\beta$ was estimated as 0.22 deg. The phase error originated from the sampling error, which depends on the frequency and the visibility of the heterodyne interference signal, the camera recording time, the frame exposure time, the frame period, and the number of gray levels.[23] Considering the related experimental conditions and the visibility of the moiré fringes with a value of 0.3, the phase error $\Delta\theta$ can be evaluated with a value of 0.32 deg. Substituting the values of Δp, $\Delta\beta$, and $\Delta\theta$, the experimental conditions, and the results into Eqs. (16)–(21), yielded a ΔR estimate of 5.81 μm.

Furthermore, the error in the thin-film stress $\Delta\sigma_f$ originating from ΔR can be derived as

$$\begin{aligned}\Delta\sigma_f &= \left|\frac{\partial\sigma_f}{\partial R}\right|\Delta R + \left|\frac{\partial\sigma_f}{\partial R_0}\right|\Delta R_0 \\ &= \frac{(Y_s t_s^2 - Y_f t_f^2)^2 + 4Y_s Y_f t_s t_f (t_s + t_f)^2}{6(1+v)Y_s Y_f t_s t_f (t_s + t_f)} \frac{Y_f^*}{\left(1 + \frac{Y_f^* t_f}{Y_s^* t_s}\right)} \\ &\quad \cdot \left[\left|\frac{1}{R^2}\right|\Delta R + \left|\frac{1}{R_0^2}\right|\Delta R_0\right], \end{aligned} \tag{22}$$

where ΔR_0 is equal to ΔR. Substituting ΔR, the experimental conditions, and the results into Eq. (22), yielded a $\Delta\sigma_f$ estimate of 7.45 MPa. According to the preceding error analysis, the proposed method has the advantages of high resolution and high accuracy, and the method can be useful

in the fabrication and development of flexible electronic devices.

4 Conclusion

This paper proposes a stress measurement system for thin films on flexible substrates by using a projection moiré method and heterodyne interferometry. The phase of the optimized heterodyne moiré signal is determined using a least-squares sine fitting algorithm, and the surface profile of the flexible test substrate is then obtained. The thin-film stress is obtained by representing the cross-sectional curve of the substrate by using a polynomial fitting method, estimating the resultant curvature radii of the uncoated and coated substrates, and using these two radii in the corrected Stoney formula. This method offers the advantages of high accuracy, high stability, high resolution, and high capacity for substrates with high flexibility and a large measurement depth.

Acknowledgments

The authors would like to thank the National Science Council of the Republic of China, Taiwan, for financially supporting this research under Contract Nos. MOST 103-2221-E-035-031 and MOST 104-2221-E-035-062.

References

1. S. R. Forrest, "The path to ubiquitous and low-cost organic electronic appliances on plastic," *Nature* **428**, 911–918 (2004).
2. K. Nomura et al., "Room-temperature fabrication of transparent flexible thin-film transistors using amorphous oxide semiconductors," *Nature* **432**, 488–492 (2004).
3. T. Someya et al., "A large-area, flexible pressure sensor matrix with organic field-effect transistors for artificial skin applications," *Proc. Natl. Acad. Sci. U. S. A.* **101**, 9966–9970 (2004).
4. G. Gustafsson et al., "Flexible light-emitting diodes made from soluble conducting polymers," *Nature* **357**, 477–479 (1992).
5. M. Berggren et al., "Light-emitting diodes with variable colours from polymer blends," *Nature* **372**, 444–446 (1994).
6. M. W. Rowell et al., "Organic solar cells with carbon nanotube network electrodes," *Appl. Phys. Lett.* **88**, 233506 (2006).
7. F. C. Krebs, S. A. Gevorgyan, and J. Alstrupa, "A roll-to-roll process to flexible polymer solar cells: model studies, manufacture and operational stability studies," *J. Mater. Chem.* **19**, 5442–5451 (2009).
8. C. Li, J. Han, and C. H. Ahn, "Flexible biosensors on spirally rolled microtube for cardiovascular in vivo monitoring," *Biosens. Bioelectron.* **22**, 1988–1993 (2007).
9. D. Simon et al., "A comparison of polymer substrates for photolithographic processing of flexible bioelectronics," *Biomed. Microdevices* **15**, 925–939 (2013).
10. M. J. Pechersky, C. S. Vikram, and R. F. Miller, "Residual stress measurements with laser speckle correlation interferometry and local heat treating," *Opt. Eng.* **34**, 2964–2971 (1995).
11. S. T. Lin, "Blind-hole residual stress determination using optical interferometry," *Exp. Mech.* **40**, 60–67 (2000).
12. C.-L. Tien, C.-C. Lee, and C.-C. Jaing, "The measurement of thin film stress using phase shifting interferometry," *J. Mod. Opt.* **47**, 839–849 (2000).
13. X. Dong et al., "Full-field measurement of nonuniform stresses of thin films at high temperature," *Opt. Express* **19**, 13201–13208 (2011).
14. C. H. Ma, J. H. Huang, and H. Chen, "Residual stress measurement in textured thin film by grazing-incidence X-ray diffraction," *Thin Solid Films* **418**, 73–78 (2002).
15. U. Welzel et al., "Stress analysis of polycrystalline thin films and surface regions by x-ray diffraction," *J. Appl. Crystallogr.* **38**, 1–29 (2005).
16. K.-S. Lee et al., "Measurement of stress in aluminum film coated on a flexible substrate by the shadow moiré method," *Appl. Opt.* **47**, C315–C318 (2008).
17. K.-T. Huang and Y.-M. Lo, "Measurement of residual stress for ITO/PET substrates by the double beam shadow moiré interferometer," *Appl. Opt.* **51**, 1566–1571 (2012).
18. M. Testorfa et al., "Talbot effect for oblique angle of light propagation," *Opt. Commun.* **129**, 167–172 (1996).
19. K. J. Gasvik, *Optical Metrology*, Chapter 7, 3rd ed., pp. 173–175, John Wiley & Sons, Ltd. (2002).
20. C. Quan, Y. Fu, and C. J. Tay, "Determination of surface contour by temporal analysis of shadow moiré fringes," *Opt. Commun.* **230**, 23–33 (2004).
21. Massachusetts Institute of Technology, "Material property database," http://www.mit.edu/~6.777/matprops/polyimide.htm (12 August 2014).
22. Massachusetts Institute of Technology, "Material property database," http://www.mit.edu/~6.777/matprops/ito.htm (12 August 2014).
23. Z.-C. Jian et al., "Optimal condition for full-field heterodyne interferometer," *Opt. Eng.* **46**, 115604 (2007).

Kun-Huang Chen received his BS degree from the Physics Department of Chung Yuan Christian University, Taiwan, in 2000 and his PhD from the Institute of Electro-Optical Engineering of National Chiao Tung University, Taiwan, in 2004. In 2004, he joined the faculty of Feng Chia University, where he is currently a professor with the Department of Electrical Engineering. His current research activities are optical metrology and optical sensors.

Jing-Heng Chen received his BS degree from the Physics Department of Tunghai University, Taiwan, in 1997 and his MS and PhD degrees from the Institute of Electro-Optical Engineering, National Chiao Tung University, Taiwan, in 1999 and 2004, respectively. In 2004, he joined the faculty of Feng Chia University, where he is currently a professor with the Department of Photonics. His current research interests are optical testing and holography.

Hua-Ken Tseng received his BS and MS degrees from the Department of Electrical Engineering of Feng Chia University, Taiwan, in 2012 and 2014, respectively. Currently, he is working at Taiwan Semiconductor Manufacturing Co., Ltd. His current research interests are biosensors and optical testing.

Wei-Yao Chang received his MS degree from the Department of Electrical Engineering of Feng Chia University, Taiwan, in 2009 and his PhD from the Institute of Electro-Optical Engineering of National Chiao Tung University, Taiwan, in 2015. Currently, he is working in Chroma Ate Inc. His current research interests are biosensors and optical testing.